SIZE EFFECT ON THROUGH-THICKNESS STRENGTH PROPERTIES OF 3D LOADED COMPOSITE LAMINATES

M. Hoffmann[1], K. Zimmermann[2], B. Bautz[3] and P. Middendorf[4]

[1]Dept. Lightweight Design & Optimization, 81663 Munich, Germany
Email: marco.hoffmann@airbus.com, Web Page: http://www.airbusgroup.com
[2]Dept. Lightweight Design & Optimization, 81663 Munich, Germany
Email: Kristian.zimmermann@airbus.com, Web Page: http://www.airbusgroup.com
[3]Dept. Lightweight Design & Optimization, 81663 Munich, Germany
Email: brian.bautz@airbus.com, Web Page: http://www.airbusgroup.com
[4] Institute of Aircraft Design, University of Stuttgart, Pfaffenwaldring 31, 70569 Stuttgart, Germany
Email: peter.middendorf@ifb.uni-stuttgart.de, Web Page: http://www.ifb.uni-stuttgart.de/

Keywords: size effect, unfolding, interlaminar tensile strength, interlaminar shear strength

Abstract
Accurate and size-dependent through-thickness strength parameters are needed for accurate failure predictions of composite load introductions. In this paper the size effect on the through-thickness strength properties of unidirectional and quasi-isotropic carbon/epoxy laminates is studied. A combined experimental and numerical approach is applied to determine accurate values of the stress levels at failure. Unfolding tests on curved beams and short beam bending tests are chosen as representative test cases. For both load cases simple analytical methods to determine the interlaminar stresses show certain drawbacks compared to the numerical models. A size effect is observed in both test cases which can be characterised by the Weibull statistical model. In addition the quasi-isotropic laminates fail at lower stress levels than the unidirectional laminates. Both effects need to be considered for the sizing of composite structures.

1. Introduction

The mass fraction of carbon fibre-reinforced plastics (CFRP) of the overall structure has risen to more than 50% with the latest generation of long-range aircrafts. Nevertheless, the application of CFRP structures is still limited by, among others, feasible load introduction concepts and reliable sizing methods. Due to the locally concentrated loads which cause complex three-dimensional (3D) stress states the sizing of load introductions of CFRP structures is a big challenge. The high load levels which are characteristic for aircraft structures can result in high laminate thicknesses, typically well above 30 mm. Possible load introductions for this type of structures are e.g. composite lugs. 3D stress states are also present in other CFRP structures, like e.g. curved laminates which are subjected to bending loads contrary to their curvature. In aircraft industries this load case is known as "unfolding" and may cause failure in curved corners, like they are present e.g. at brackets or omega frames. In contrast to classical applications of CFRP laminates in thin-walled structures, where a plane stress state can be assumed, the out-of-plane components of the stress tensor cannot be neglected for this type of structures. They may even trigger failure due to the absence of reinforcements in thickness direction which results in low strength parameters. Sizing methods need to take into account this type of failure and therefore accurate strength properties in thickness direction are needed.

The work presented in this paper is part of the publically funded research project MAI Last. Within this project a building block approach is applied to generate design guidelines for load introductions of

Excerpt from ISBN 978-3-00-053387-7

CFRP structures. Starting on coupon level, novel specimen geometries have been developed to determine accurate strength parameters under interlaminar tensile and shear loading (see e.g. [1]). In the next step a combined experimental and numerical approach is applied to validate the strength parameters by testing and stress analyses of generic specimens on element level. Two representative test cases have been chosen, which lead to failure under interlaminar tensile (ILT) and interlaminar shear (ILS) loading, respectively. To analyse the failure behaviour under interlaminar tensile loading, unfolding tests with a triple curved beam specimen have been conducted, while three-point bending test on short beams have been picked to analyse interlaminar shear failure.

In various technical publications, like e.g. [2, 3], a size effect on matrix-dominated strength parameters of fibre-reinforced plastics with relatively brittle matrix systems has been observed, which needs to be considered in reliable sizing methods. The size effect is often explained by the Weibull statistical model [4]. This model assumes that the strength of a brittle material is controlled by the presence of flaws which are statistically distributed [2]. Following this model, the probability of flaws increases with the stressed volume of the material, which results in a reduced strength. To verify the size effect on the interlaminar strength properties of the carbon/epoxy laminates investigated in the present work, the generic specimens on element level have been manufactured with three different laminate thicknesses. The test results are combined with detailed FE analyses to determine the stress state at failure.

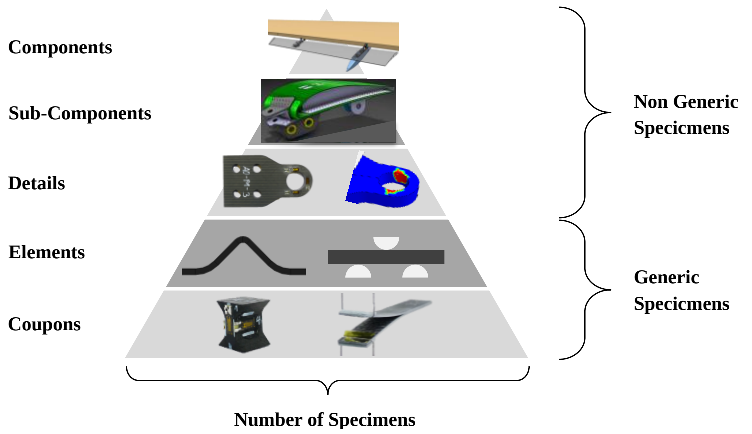

Figure 1. Building block approach.

2. Specimen geometry and manufacturing

The triple curved beam shown in Fig. 2 has been chosen to analyse the failure behaviour under ILT loading. The specimen is representative for load bypasses in several aircraft applications like e.g. fittings, brackets or omega frames. In the region of interest (ROI) the specimen features a 90° angle with a relative small radius of curvature. Due to the plane legs of the specimen in the load introduction area the specimen can easily be mounted to the clampings of a universal testing machine without any additional test fixture. During the test, the curved section in the region of interest is bended contrarily to its curvature, which causes an ILT stress with a maximum level close to the symmetry plane of the laminate (see Fig. 2).

Excerpt from ISBN 978-3-00-053387-7

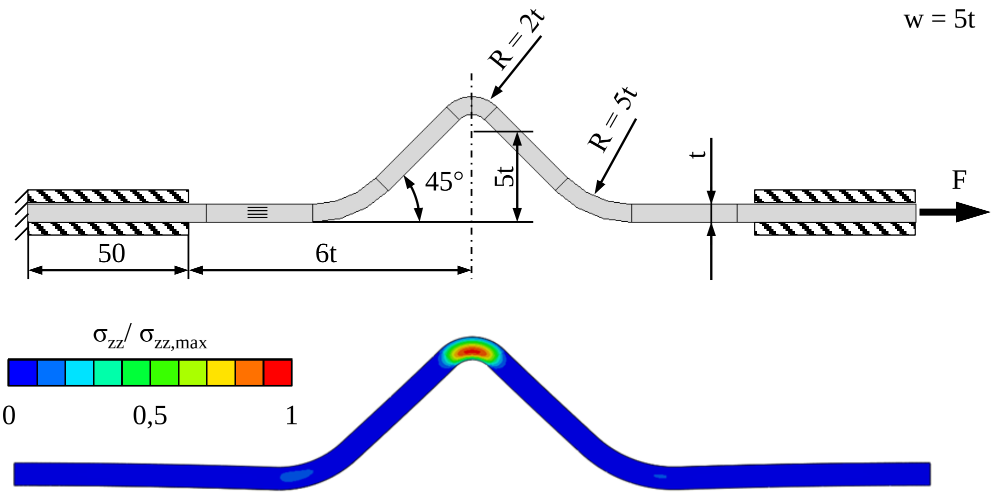

Figure 2. ILT specimen: parametrized geometry (top) and ILT stress distribution (bottom).

The failure behaviour under ILS loading has been analysed by three-point bending tests on short beam specimens adapted from DIN EN 2563 or ASTM D 2344, respectively (see Fig. 3). The application of this test method as coupon test to determine the interlaminar shear strength of composite laminates is often criticised due to the complex stress state in the specimen, which is composed of interlaminar shear stress, bending stresses and contact stresses close to the rollers. Due to the simplicity of the test and the combination with finite element analyses to determine the stress state within the failure area it is considered as suitable test method on element level in the present study.

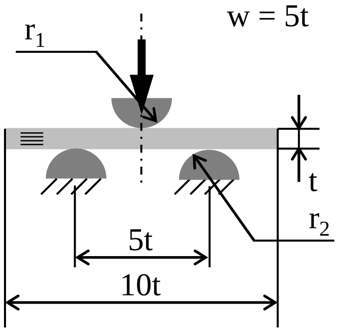

Figure 3. ILS specimen geometry.

Table 1. Dimensions of rollers for ILS tests.

t (mm)	r_1 (mm)	r_2 (mm)
2,0	1,5	1,5
5,0	6,0	3,0
10,0	12,0	3,0

To analyse the presence of a size effect on through-thickness strength parameters both the ILT and ILS specimens have been manufactured with three different nominal laminate thicknesses of 2 mm, 5 mm and 10 mm. To ensure comparable stress ratios in the specimens of different size all geometric parameters have been parameterised by the laminate thickness t. In the case of the ILS tests the radii of the rollers were also adapted to the size of the specimens (see Table 1). The ILT and ILS specimens of the same thickness have been manufactured in one shot. The triple curved plates have been manufactured from non-crimp fabrics of HTS carbon fibres and the epoxy resin Hexcel RTM6 in a vacuum assisted resin infusion process (VAP) with a male tool. Two different layups have been analysed. A unidirectional layup has been applied for specimens with a thickness of 2 mm and 5 mm (test series UD-T2 and UD-T5), while a quasi-isotropic layup has been applied for all of the considered thicknesses (test series QI-T2, QI-T5 and QI-T10). For statistical reasons each test series consists of five specimens.

Excerpt from ISBN 978-3-00-053387-7

3. Interlaminar tensile tests

The ILT tests have been carried out on a 10 kN capacity uniaxial universal testing machine at an extension rate of 1 mm/min. Every specimen has been instrumented with a strain gauge with a gauge length of 6 mm on the outer radius of the region of interest (see Fig. 4). The tests have been cancelled after initial failure occurred in the form of a delamination close to the symmetry plane in the region of interest which has been characterized by a sudden load drop. The progressive failure of some ILT specimens which have been loaded up to final failure was already presented in [6] and will not be addressed in this paper, since only the initial failure load is needed to draw conclusions about the ILT strength.

A first evaluation of the maxim ILT stresses $\sigma_{zz,max}$ at initial failure has been done by the analytical approach of [5]. The approach was developed by using simple bending theory. The load P_{max} at initial failure as well as geometrical parameters like the cross section *wt* in the region of interest, the cantilever *h* and the inner (r_i) and outer radius (r_o) of the 90° angle are applied to determine the maximum ILT stress according to equation (Eq. 1). An overview of the determined maximum ILT stresses at initial failure is given in Table 2. If test series ILT-QI-T2 is excluded, a clear size effect on the ILT strength can be observed for both layups. If the laminates with a thickness of 5 mm are considered, the layup seems to have a limited effect on the ILT strength.

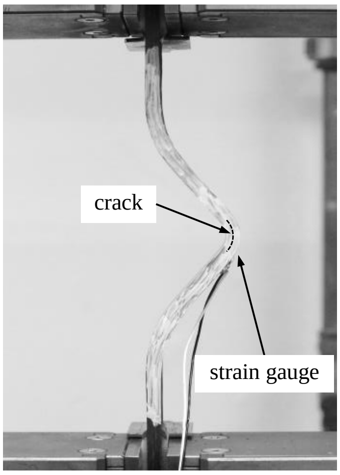

Figure 4. ILT test setup.

Table 2. Overview of ILT test results.

Test series	$\sigma_{zz,max}$	
	$\bar{x}$ (MPa)	*CV* (%)
ILT-UD-T2	73,4	10,6
ILT-UD-T5	64,4	3,9
ILT-QI-T2	44,7	6,8
ILT-QI-T5	67,5	9,1
ILT-QI-T10	55,1	3,8

$$\sigma_{zz,\max} = \frac{3}{2}\frac{F_{\max} h}{wt\sqrt{r_i r_o}} \quad (1)$$

4. Interlaminar shear tests

Due to the higher level of expected failure loads the ILS tests have been performed on a 100 kN capacity uniaxial universal testing machine which has been equipped with a three-point bending test rig (see Fig. 5). The specimens have been loaded with an extension rate of 1 mm/min. Prior to each test series a calibration curve has been determined with a steel beam to capture the compliance of the test rig. All specimens have been loaded up to initial failure in the form of a delamination close to the symmetry plane of the laminate, which has resulted in a sudden load drop.

Excerpt from ISBN 978-3-00-053387-7

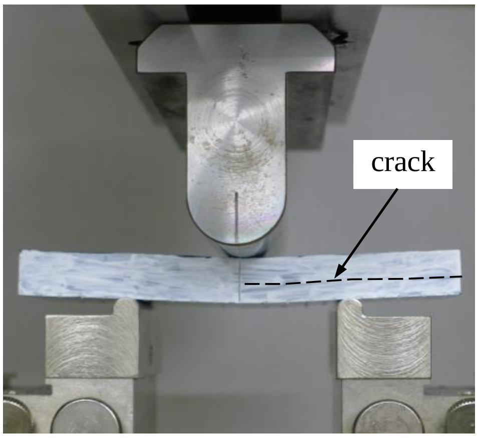

Figure 5. ILS test setup.

Table 3. Overview of ILS test results.

Test series	$\tau_{xz,max}$ $\bar{x}$ (MPa)	$\tau_{xz,max}$ *CV* (%)
ILS-UD-T2	76,8	7,5
ILS-UD-T5	66,0	2,0
ILS-QI-T2	47,4	8,2
ILS-QI-T5	44,9	4,8
ILS-QI-T10	42,5	4,9

A first estimation of the maximum ILS stresses $\tau_{xz,max}$ at the initial failure load P_{max} has been done by (Eq. 2), which was originally proposed to estimate the maximum shear stress within the cross section of width *w* and thickness *t* of an elastic, homogenous and isotropic beam. The analytically determined maximum ILS stresses at failure are summarized in Table 3. In general, a decrease of the maximum ILS stresses could be observed with increasing laminate thickness. In addition, the unidirectional laminates fail at significantly higher ILS stress levels than the quasi-isotropic laminates of the same thickness.

$$\tau_{xz\max} = \frac{3}{4}\frac{P_{\max}}{wt} \tag{2}$$

5. Numerical stress analyses

5.1 Modelling method

The commercial FE code Abaqus/Standard has been applied for the numerical analyses. The stress state at initial failure should be evaluated for every single specimen. Therefore, automated by a script, a model has been set up for every single specimen with its detailed geometrical dimensions. A force-controlled loading up to the initial failure load has been applied. The specimens have been modelled by 3D continuum elements. The element size has been adapted to the size of the specimen. Thus, a size-independent number of elements has been chosen for each dimension of the specimens. In thickness direction this has resulted in a number of 2 elements per UD layer for a laminate thickness of 2 mm and of 2 UD layers per element for a laminate thickness of 10 mm. The constitutive behaviour of each layer has been defined by the linear elastic orthotropic material model given in Table 4.

Table 4. Elastic material properties of a UD layer of HTS/RTM6.

E_{11} (GPa)	$E_{22} = E_{33}$ (GPa)	$G_{12} = G_{13}$ (GPa)	G_{23} (GPa)	$\nu_{12} = \nu_{13}$ (1)	ν_{23} (1)
120,0	8,6	4,5	2,9	0,30	0,26

5.2 Stress analyses of the ILT tests

Excerpt from ISBN 978-3-00-053387-7

The force-controlled load application as well as the boundary conditions at the fixed end of the specimen have been applied at node sets, which represent the beginning of the clamped region. The nonlinear effect of large deformations has been considered by the analyses to account for the reduction of the bending moment within the region of interest due to deflection of the specimens during the test. Prior to the evaluation of the stress state the correlation of the global force-displacement behaviour and of the strain within the gauge section of tests and analyses has been checked to validate the numerical models. In all of the models the maximum ILT stress is located in the centre of the 90° angle, close to but not within the symmetry plane of the laminate (see Fig. 6). The determined maximum ILT stresses within the specimen at initial failure loads are summarized in Table 5. In general, the numerically determined ILT stresses are significantly lower than the ones determined analytically by (Eq. 1), which is caused by the consideration of geometric nonlinearity in the FE analyses. Nevertheless both determinations lead to the same conclusions regarding the general effects of size and layup on the ILT strength.

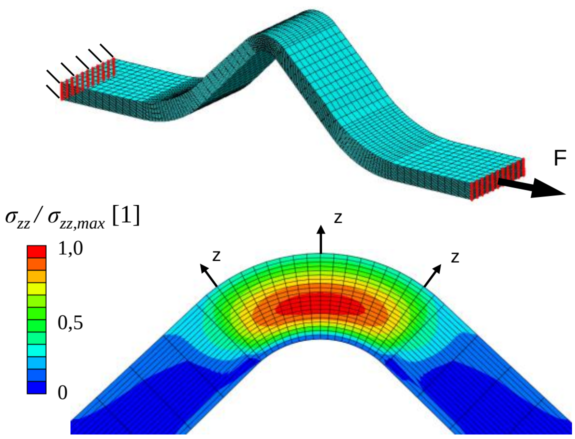

Figure 6. Setup and stress distribution of ILT FE model.

Table 5. ILT strength determined by FEA.

Test series	$\sigma_{zz,max}$ $\bar{x}$ (MPa)	CV (%)
ILT-UD-T2	40,3	12,9
ILT-UD-T5	38,9	3,8
ILT-QI-T2	29,0	6,8
ILT-QI-T5	44,3	9,3
ILT-QI-T10	37,7	3,5

5.3 Stress analyses of the ILS tests

Only a quarter of the ILS specimen has been modelled and symmetry conditions have been applied to increase the computational efficiency of the models. The boundary conditions of the bearings and the load introduction have been applied at the corresponding nodes. Due to the high shear deformation of the elements within the region of interest, quadratic 20-noded continuum elements with reduced integration points have been applied to avoid shear locking. With this type of elements the force-displacement curves of tests and FE analyses show a good correlation. In the FE models the maximum ILS stresses are present at the load introduction areas, which is partially caused by the simplified boundary conditions. Since the failure occurred within the shear stress fields between stamp and bearings, the peak stresses in the load introduction areas were ignored. The selected region for the determination of the maximum ILS stresses is given in Fig. 7. Table 6 gives an overview of the determined maximum ILS stresses at initial failure load. In most of the cases there are only small deviations between the analytically and numerically determined values for the maximum ILS stresses. The negative effect of an increasing laminate thickness on the maximum ILS stresses was confirmed by the numerical analyses.

Excerpt from ISBN 978-3-00-053387-7

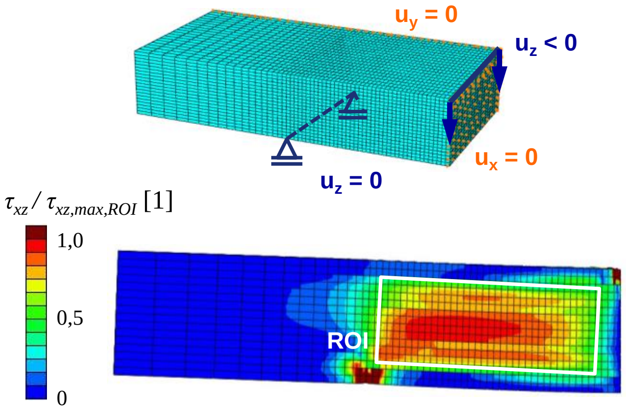

Figure 7. Setup and stress distribution of ILS FE model.

Table 6. ILS strength determined by FEA.

Test series	$\tau_{xz,max}$ $\bar{x}$ (MPa)	$\tau_{xz,max}$ CV (%)
ILS-UD-T2	72,3	7,8
ILS-UD-T5	63,2	1,3
ILS-QI-T2	54,3	8,0
ILS-QI-T5	43,9	4,8
ILS-QI-T10	42,4	4,9

6. Discussion of the size effect

The Weibull statistical model [4], which assumes that the strength of brittle materials is controlled by the presence of flaws, which are statistically distributed within the material, is often applied to describe size effects on the strength properties of composite materials. Based on this model, Hitchinson et al. [3] derived the following realtionship (Eq. 3) between strengths (R_k) and volumina (V_k) or thicknesses (t_k) of geometrically identical specimens subjected to identical loading conditions [2]. The parameter m is the Weibull modulus, which is assumed to be a measure of the variability of the material and has to be adapted to the test data. Following [3] it can be related to the coefficient of variation of the experimentally determined strength by equation (Eq. 4).

$$\frac{R_1}{R_2} = \left(\frac{V_1}{V_2}\right)^{\frac{1}{m}} = \left(\frac{t_1}{t_2}\right)^{\frac{3}{m}} \qquad (3)$$

$$m = \frac{1,2}{CV} \qquad (4)$$

If the test data can be characterized by (Eq. 3), a log-log plot of strength versus thickness should give a straight line. In Fig. 8 the log-log plots of ILT and ILS strength determined by the combined experimental and numerical approach are given. In all cases the Weibull modulus (see Table 7) has been determined by a least square fit to the mean values of strength. The results for a QI laminate with a nominal thickness of 2 mm under ILT loading have been excluded due to the unreasonable low stress level at failure, which could not be explained and might have been caused by manufacturing induced defects. In general, the application of the Weibull theory gives a good estimation of the size effect on the mean values of ILT and ILS strength in the current study. For most of the test series, except ILT-T2-UD, the single test data lies within the range of the CV expected by equation (Eq. 4). There is also an effect of the layup on the determined strength. Under ILS loading the UD laminates show a higher strength compared to the QI laminates for all thicknesses. If the Weibull modulus follows the assumptions to be constant and be a material parameter, this effect should also be present for the ILS strength of laminates with a thickness of more than 10 mm. If the Weibull fits under ILT loading are considered, the UD laminates show a higher strength at laminate thickness of less than 10 mm. At a laminate thickness of 10 mm the strength of UD and QI laminates is expected to be coincident. But this is only a guess by extrapolation and should be validated by further test series. A possible reason for the mostly lower strength of the QI laminates is the restriction of free transversal contraction, caused by the adjacent layers of different orientation. Compared to UD laminates this restrictions result in a more complex, non-uniform stress state and failure under mixed-mode loading conditions.

Excerpt from ISBN 978-3-00-053387-7

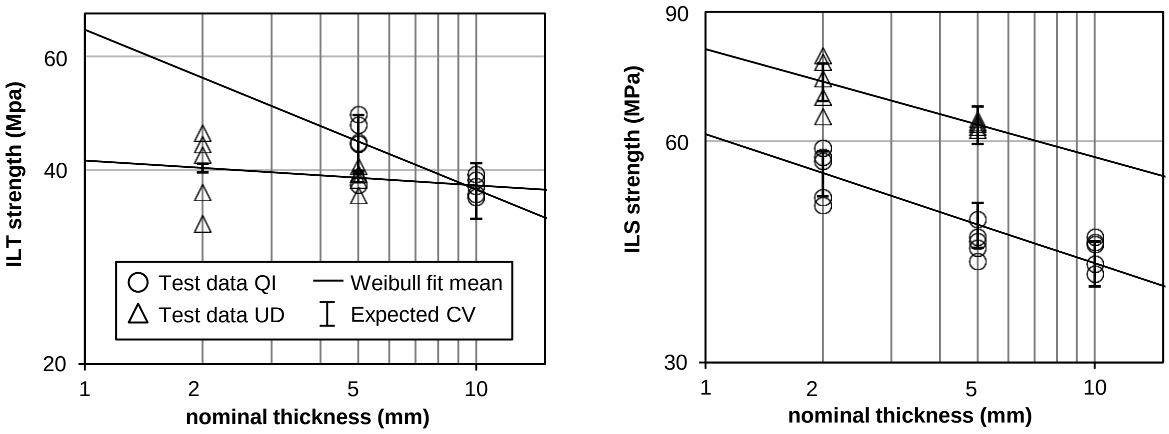

Figure 8. Effects of laminate thickness on ILT strength (left) and ILS strength (right).

Table 7. Weibull moduli of ILT and ILS strength.

	ILT strength		ILS strength	
Layup	UD	QI	UD	QI
m (1)	77,8	12,1	20,4	17,1

6. Conclusions

In this paper a set of test series on CF/epoxy laminates with two different layups (UD, QI) and three different laminate thickness (2 mm. 5 mm, 10 mm) under ILT and ILS loading has been presented. The test methods include unfolding tests of curved beams and three-point bending tests on short beams. The maximum stresses at initial failure have been evaluated by analytical as well as numerical methods. In the case of interlaminar shear loading the analytical approach already gives a good estimation of the ILS strength, especially if the laminate can be treated as a homogenous material, which was the case for all UD laminates and the QI laminates with a thickness of at least 5 mm. In contrast to that, the analytical and numerical estimations of the ILT strength of the curved beam specimens show a big difference, which was already observed in [5] for specimens with comparable low ratios of curvature radius to laminate thickness. Reasons for these differences are the neglect of geometrical nonlinearity in terms of the changing curvature and offset between the load vector and the curved section as well as the anisotropy (regarding in-plane and out-of-plane elastic properties) and inhomogeneity of the laminates.

The presence of a size effect on the ILT and ILS strength of carbon/epoxy laminates has been confirmed by the presented test series. If a few exceptions are ignored, the Weibull theory seems to be fitted to characterize this size effect. In addition, the layup has an effect on the ILT and ILS strength of laminates. Due to the inhomogeneity of the laminate the layers and interfaces of QI laminates are exposed to more complex stress states than the ones of UD laminates, which results in failure at a lower level of ILT or ILS stress, respectively. The effects of size and layup need to be considered for accurate failure predictions of composite structures on higher levels of the building block approach. To derive a reliable estimation of the size effect on ILS and ILT strength the database should be extended to further combinations of layups and laminate thicknesses, especially in terms of thicknesses which are representative for highly loaded aircraft structures (t $\geq$ 30 mm). Nevertheless, the determined Weibull moduli can give a first estimation of the ILT and ILS strength of thick carbon/epoxy laminates. Therefore they will be applied to predict the failure behaviour of composite lugs under out-of-plane loading conditions in ongoing studies.

Excerpt from ISBN 978-3-00-053387-7

Acknowledgments

The support of the German Federal Ministry of Education and Research (BMBF) and the Bavarian Ministry of State for Economics, Media, Energy and Technology in the project MAI Last, as part of the leading-edge cluster MAI Carbon, is gratefully acknowledged. The authors also wish to thank Kurt Pfeffer for the mechanical testing activities.

References

[1] M. Hoffmann, K. Zimmermann, B. Bautz and P. Middendorf. A new specimen geometry to determine the through-thickness tensile trength of composite laminates. *Composites Part B*, 77:145-152, 2015.
[2] W. Cui, M. Wisnom and M. Jones. Effect of specimen size on interlaminar shear strength of unidirectional carbon fibre-epoxy, *Composites Engineering*, 4: 299-307, 1994.
[3] J. Hitchon and D. Phillips. The effect of specimen size on the strength of CFRP, *Composites*, 9: 119-124, 1978.
[4] W. Weibull. A statistical theory of the strength of materials, Scientific Report, KTH Stockholm, Sweden, 1939.
[5] K. Kedward, R. Wilson and S. McLean. Flexure of simply curved composite shapes, *Composites*, 20: 527-536, 1989.
[6] M. Hoffmann, K. Zimmermann and P. Middendorf. Determination of the through-thickness strength properties to predict the failure of thick-walled composite lugs. *Proceedings of the 20th International Conference on Composite Materials ICCM-20, Copenhagen, Denmark,* July 19-24 2015.

Excerpt from ISBN 978-3-00-053387-7